INTERNATIONAL JOURNAL OF SOCIAL HEALTH
https://ijsh.ph/index.php/rp
Volume 2 Number 9 September 2023 E-ISSN: 2984-7079

ANALYSIS OF VARIATION OF TIN FILTER ON NOISE VALUES IN CT SCAN MASTOID PROTOCOL USING CT SCAN SINGLE SOURCE: PHANTOM STUDY

Merry Suzana[1], Kusworo Adi[2], Darmini[3]
Politeknik Kesehatan Kemenkes Semarang, Jawa Tengah, Indonesia
merrysuzana@gmail.com

KEYWORDS
ct scan mastoid, tin filter, noise, snr, nps, indoqct.

ABSTRACT
Since its introduction in 1972, CT Scan technology has developed rapidly from year to year, especially in reducing radiation dose; various technologies have been developed, including dual-energy or dual source technology with a technique of only a quarter of the gantry rotation. The aim of this research is to find out and analyze tin filter variations on noise in the mastoid CT scan protocol using a single source CT scan: phantom study. The method used in this research is Pre-Experimental with Posttest-Only Control Design. The noise value research results showed a difference in noise and SNR values with a p-value ($p<0.05$), and there was a reduction in radiation dose of 41.95% compared to the standard protocol. NPS values are at a frequency of 0.28, except for the Sn100 protocol. Subjective Analysis by two radiologists with a kappa value of 0.75 indicated that there was a moderate level of agreement. The Tin Filter Sn100 protocol can reduce the radiation dose, and the resulting image quality is good enough for diagnostic purposes, so the Tin Filter Sn100 protocol can be used as a Standard Operational Procedure for Mastoid CT Scan examination at Hermina Depok Hospital. This study has implications that may contribute to refining mastoid CT scanning protocols, leading to improved image quality, reduced radiation exposure, and improved diagnostic capabilities in clinical practice.

DOI: 10.58860/ijsh.v2i9.92

Corresponding Author: Merry Suzana
E-mail: merrysuzana@gmail.com

INTRODUCTION

Since its introduction in 1972, CT Scan technology has developed rapidly from year to year, especially in reducing radiation dose; various technologies have been developed, including dual-energy or dual source technology with a technique of only a quarter of the gantry rotation. Can produce images that can be processed so that the X-ray exposure time can be reduced, and then the radiation dose released can be reduced by up to a quarter of a percent (Ertel et al., 2009; M. Lell et al., 2009; Leschka et al., 2009; Tacelli et al., 2010), and some have developed filter back projection reconstruction techniques or what is known as iterative reconstruction to adapt low dose images that are identical to rough or noisy images. (Kalmar et al., 2014; Singh et al., nd) . Software technology such as Automatic Tube Current Modulation has also been developed; this software can reduce the radiation dose during CT Scan examination exposure. This technology automatically adjusts the tube current (mA) and adjusts attenuation variations in the patient's body when the X-ray tube rotates from various angles, known as angular tube current modulation (Mannudeep K. Kalra, Michael M. Maher, Thomas L. Toth, Bernhard Schmidt, Bryan L. Westerman, Hugh T. Morgan, 2004; McKenney et al., 2014; Mcnitt-gray, 2011). All of these radiation dose reduction technologies are very useful in scanning organs with high radiosensitivity, including the organs in the head area.

The organs in the head area have a high level of density, so in practice, the CT Scan examination carried out on this part of the head requires quite a large dose; apart from that, there are also parts of the organ that require High-Resolution image quality to make a diagnosis—a for example, in the mastoid air cell organ (Dexian Tan et al., 2018). Mastoid Air Cells are small spaces filled with air located in the mastoid process of the temporal bone. These cells are part of the middle ear and are important for regulating air pressure in the ear (Magnuson, 2003). The Mastoid Air Cell organ is close to organs that have radiosensitive properties, such as the eye lens (Sowby, 1981) and the thyroid gland. It has been researched that X-ray exposure in radiodiagnostics can increase the risk of microcarcinoma in the thyroid organ (Kovalchuk & Kolb, 2017). Therefore, during CT scanning, This mastoid air cell scan requires great care in determining the radiation dose used in the examination, and this radiation dose is very closely related to the quality of the resulting image.

These image qualities include Spatial, Contrast, and Temporal Resolution (Romans, 2011). Of these three image qualities, the most influential when the CT scan image is underexposed is Contrast Resolution. This Contrast Resolution can be assessed with a phantom containing objects; distinguishing very small objects is difficult to do subjectively. Therefore, noise is important in detecting large images—low-contrast resolution. Noise, SNR, and NPS are the most complete analyses in terms of low-contrast resolution (SEERAM, 2016).

In 2017, a patient pre-filter system was developed by Siemens Healthiners on the Single Source CT Scan system, marketed under Tin Filter (Braun et al., 2015). This Tin Filter is the development of a pre-patient system on the previous system known as the bowtie filter; this bowtie filter is the basic filtration in the CT Scan system, which is useful in forming X-ray beams. The principle of the Tin Filter is the same as when we look at the sun with and without glasses; of course, it will be easy to see the sunlight with glasses clearly to eliminate the dazzling effect. Tin Filter or Sn filter, Sn comes from the Latin word for tin, namely stanum. The Tin Filter is an additional filter placed in front of the bowtie filter to filter the beam from the X-ray tube before it hits the patient's body. As a result, only high-energy photons reach the patient, while very low energy will not be able to penetrate this tin filter will not reach the patient and will be filtered so that the radiation dose can be suppressed (Choi et al., 2020; Hamann et al., 2017; MM Lell et al., 2015; Rajendran et al., 2020), by producing high photon energy can reduce noise and contrast in the image, although this filter method can reduce exposure to ionizing radiation reaching the patient, noise in the image has an important role in terms of image quality and diagnostic performance (Mozaffary et al., 2019). This tin filter has a selection variation according to the energy level used between Sn100, Sn110, Sn120, and Sn140; Sn indicates the use of tin filters. For example, Sn100, at 100 kV energy, uses tin filters as energy filters (Schüle et al., 2023).

In recent years, there have been studies related to lead filters on CT scans with multiple sources on Thorax CT scan examination with Covid diagnosis with lead filters using Sn150 kV studied by researchers (Agostini et al., 2021) . In 2020 researchers with low-dose CT results with spectral and ADMIRE3 formation were able to produce acceptable image quality for the evaluation of Covid19 patients and significantly reduce dose and movement artifacts (Agostini et al., 2021) . The use of tin filters on Sn100 kV and Sn140 kV at the shoulder joint by Yun Seok Choi et al. 2020 (Choi et al., 2020) with the results of Shoulder CT Scan with Sn140 kV can reduce radiation dose by around 70 – 60% and image noise when maintaining contrast images compared to conventional protocols, Tin filter with a combination of the high pitch in detecting ureteral stones by Gu Mu Yang Zhang et al. in 2017 (Zhang et al., 2017) with the results of high pitch C T Scan Pelvic Abdomen at Sn150kV can substantially reduce radiation exposure when detecting stones in the urinary tract, and the application

of dose reduction and diagnostic performance of tin filters in colorectal cancer patients by Koichiro Kimura et al. in 2022 (Kimura et al., 2022) with the results of a 100 kV tin filter can reduce the radiation dose by around 89% compared to the standard 120 kV protocol.

Hermina Depok Hospital has just installed the latest CT Scan, and there is a pre-system filter in this CT Scan system. This is the first time it has been embedded in a single-source CT Scan system, which previously only existed in dual-source systems; this new filter system can reduce the radiation dose by around 89% (Kimura et al., 2022), with a dose that is reduced quite drastically, of course, it would be a shame if it is not used properly, however, if the radiation dose is reduced so drastically, radiographers are still unsure. Using the Tin Filter will increase image noise, which is caused by reducing the number of photons reaching the photo object. Noise itself has an important role in terms of image quality and to know for sure the results of the image provided and how well it is in reducing the radiation dose with image noise that is still within tolerance limits in diagnosing an abnormality in the mastoid air cells. An inspection of Mastoid air cells is required to show the smallest structures of these organs so that they can be seen well, especially the bones, malleus, and incus. Several radiologists at Hermina Hospital Depok complained about this mastoid examination for small bone parts that are blurry and somewhat unclear in that area; this examination is carried out quite a lot for around 25% of the total patients every month. Therefore, high-resolution image quality is required to establish a proper diagnosis. The weakness of the standard bowtie filter pre-filter system is that the output beam resulting from the collision is still mixed with super low energy and other energies; therefore, organs with a high-density level in their smallest structures will result in blooming artifacts. In contrast to the tin filter principle, whose function is only to filter low energy and pass only high energy used in scanning. This may be useful in scanning organs with a high level of density to determine the quality of the image produced and the level of noise produced by each variation of filter tin given in the Mastoid CT Scan protocol, considering that examinations using radiation must be as efficient as possible and must conform to the ALARA principle.

Based on the background that has been written, it is very interesting to carry out a more in-depth noise analysis regarding the levels of noise values, Signal-to-Noise (SNR) and Texture Noise Power Spectrum (NPS) and the resulting dose reduction for each tin filter variation (Sn100, Sn110, Sn120 and Sn140) with the mastoid protocol on a water phantom object as a baseline image, then scanned again with a rando phantom which has specifications similar to a real human body. This is interesting to research; what causes the noise produced at each energy still needs to be widely known, and previous studies only examined one or two tin filter variations. Apart from that, this tin filter system is something new in the single source CT scan system, and of course, with a reduced radiation dose, it will produce low noise, which is very contrary to the principle that if the radiation dose is low or underexposed, you will get high noise and things like this can reduces diagnostic performance. This research will be used as the basis for making the Mastoid CT Scan Protocol SOP Low Dose. So, the aim of this research is is to find out and analyze tin filter variations on noise in the mastoid CT scan protocol using a single source CT scan: phantom study.

METHOD

Pre-Experimental Research with a Posttest-Only Control Design. This research began with scanning Water Phantom in standard protocol and followed by scanning variations of Tin Filter (Sn100, Sn110, Sn120, and Sn140), then assessed for noise and SNR. Noise texture or NPS was analyzed using indoQCT Version 22 software. Then, after getting a baseline picture of which protocol

is good, the protocol is used as a scanning protocol with phantom random objects, and interobserver agreement is calculated.

This research begins by preparing the Go Top and Water Phantom CT scan planes. Then, adjust the position of the water phantom on the examination table guided by the horizontal collimation lamp and the longitudinal collimation lamp. Position the water phantom in the middle and set the gantry tilt to 0°. Data was collected by scanning the water phantom without using a Tin Filter and Tin Filter variations (Sn100, Sn120, Sn140). Set the exposure parameters on the Siemens Somatom Go Top console table. In accordance with the mastoid examination protocol, namely with kV according to Sn Filter variations, mAs with Automatic Tube Control Modulation, tube rotation 0.6 seconds, detector collimation width 1.2 mm, image thickness 1.5 mm, B41s kernel. Scanning is done from top to bottom, starting by making a program. Researchers took scanning using an axial technique, taking several variations of Sn Filter with each series taking ten slices from the water phantom at slice numbers 12, 24, 36, 48, 60, 72, 84, 96, 108, and 120 and taking images of the water phantom without using tin. Filter by providing an un-checklist in the enable/unenable and scanning dialog boxes, and by using Tin Filter by selecting the Sn Filter variation that will be used Sn100, Sn110, Sn120, and Sn140. Next, the image resulting from the radiation is stored on the workstation. Next, the image is analyzed and measured; noise and SNR values by taking ROI (region of interest) are taken at points referring to Figure 1—Region of Interest (ROI) Measurement Points.

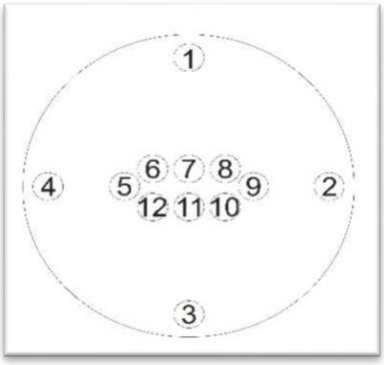

Figure 1. ROI Measurement Point

In addition, noise evaluation was also carried out using the second measurement NPS method, namely noise using the Noise Power Spectrum method using IndoQCT software in terms of the size of the noise and the texture of the noise itself, and the third Analysis, namely the radiation dose in the form of CTDIvol with units of mGy recorded on the workstation. After getting the analysis results and getting a good idea of the Tin Filter protocol, the protocol is used for scanning phantom rando, which has specifications similar to the original human body. Apart from that, noise evaluation was also carried out using the NPS method, the second measurement was noise using the Noise Power Spectrum method using IndoQCT software in terms of the amount of noise and the texture of the noise itself, and the third Analysis was radiation dose in the form of CTDIvol in mGy units recorded on the workstation. After getting the analysis results and getting a good idea of the Tin Filter protocol, the protocol is used for phantom rando scanning, which has specifications similar to the original human body in Figure 2.

Figure 2. Phantom Rando

Then, the image quality from the results of the phantom rando scanning is analyzed subjectively by a radiologist at the hospital who will apply the Mastoid Low Dose Protocol SOP.

RESULTS AND DISCUSSION

True -Experimental research has been carried out with the Posttest-Only Control Design. This research was carried out by scanning two types of phantoms, namely water phantom and rando phantom, to look for good image quality, which will be used as a new protocol and SOP for Low Dose Mastoid CT scan examinations. This research was conducted at Hermina Hospital, Depok, with data collection in April 2023.

This study used images taken from water phantom scanning; the scanning was carried out five times with standard protocols/without filter tin, Sn100, Sn110, Sn120, and Sn140. From each of these protocols, 124 images were obtained, and then ten images were selected as samples representing each area level in the water phantom, namely the edge area. Next, ten images from each standard protocol, Sn100, Sn110, Sn120, and Sn140, had their noise values measured at 12 measurement points, as in Figure 4.2. These 12 points were taken because, at each point, the area in the ROI produced a different value. Therefore, 12 different points were taken in the hope that they could represent each area in the center and other edges, and in this selected image, there were no artifacts to make it easier in the analysis process, namely in slices 12, 24, 36, 48, 60, 72, 84, 96, 108 and 120. The following are the results of scanning water phantoms obtained on the standard protocol (a), Sn100 protocol (b), Sn110 protocol (c), Sn120 protocol (d), and the Sn140 (e) protocol, as shown in Figure 3.

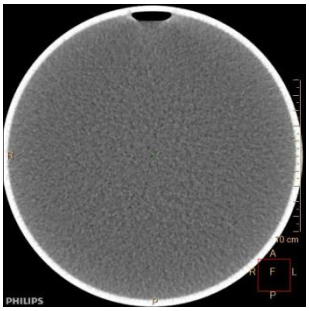

a

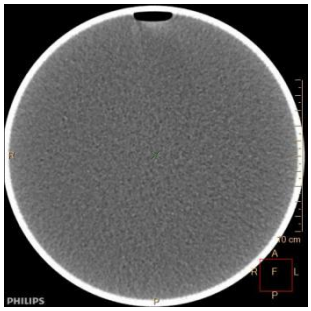

b

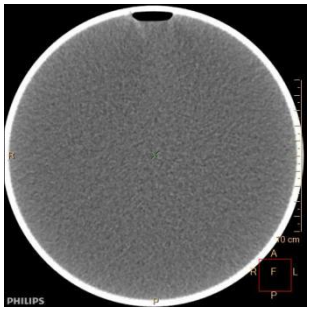

c

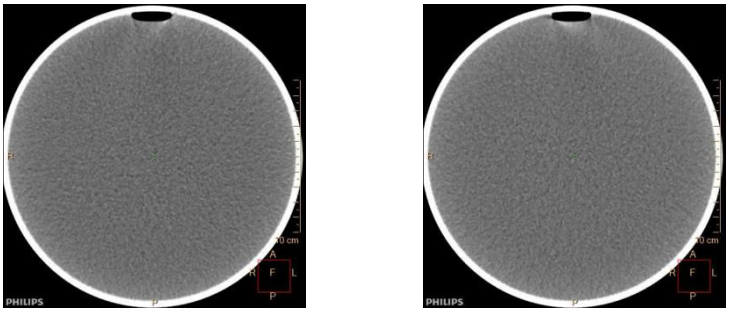

d e

Figure 3. Water Phantom Scanning Results

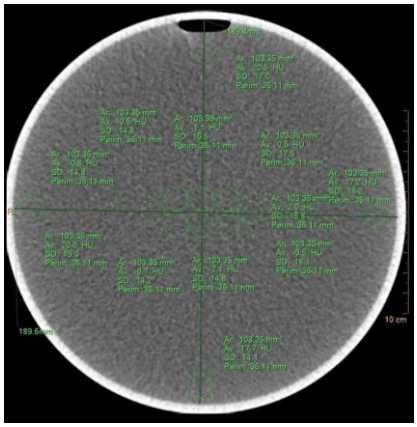

Figure 3. Twelve Noise and NSR Value Measurement Points

After being measured using ROI (region of interest), the measured noise value is obtained from the standard deviation of the ROI measurement. Then, the 12 measurement points are averaged. The noise values of the ten images in each image from each protocol are averaged with the following results:

Table 1 . Noise Value of Each Tin Filter Protocol

Protocol	N	Noise Average	Standard Deviation	Min Value	Maximum Value
Standard	10	14.0600	0.40729	13,43	14.71
sn100	10	14.5990	0.34323	14,11	15,13
Sn110	10	13.5380	0.22744	13.23	14.03
sn120	10	12.7190	0.20760	12.34	13.05
Sn140	10	12.6670	0 .29010	12.21	13.03

From Table 1, it can be seen that in the standard protocol, the average noise value is 14.0600. From each tin filter protocol, the lowest average *noise value* is in the Sn140 protocol of 12.6670, and the highest average *noise value* is in the Sn100 protocol of 14.5990.

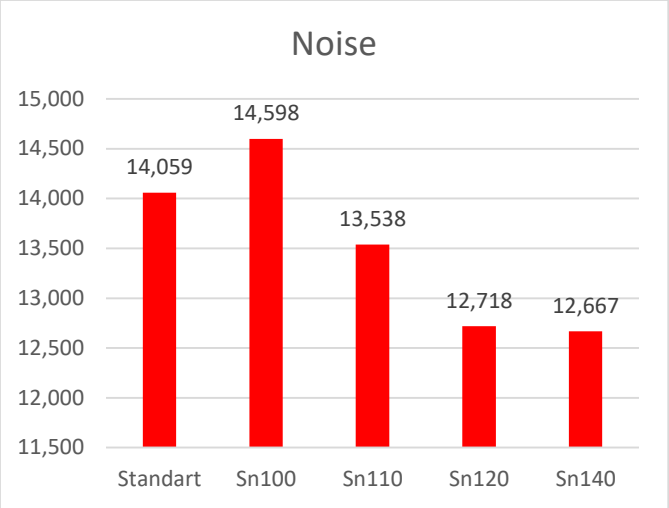

Figure 5. Noise

From Figure 5, it can be seen that in the standard protocol, the noise value is 14.059. In the tin filter variation protocol, the highest noise value produced was in the Sn100 protocol at 14.598, and the lowest was in the Sn 140 protocol at 12.667. The use of variations in the filter shows that as the energy used increases, the noise value decreases from Sn100 to Sn140. Then, the ANOVA test was continued on each Tin Filter protocol with a sig value of 0.000<0.05, so it can be concluded that the average noise value of these five Tin Filter protocols is significantly **different.** Then, proceed with post hoc ANOVA to analyze each variance between groups. In this experimental research, only the average noise values of the Sn140 and Sn120 protocols are the same, while the average noise values in the other protocols are different; thus, the Tin Filter variable The noise value only has a significant effect on the Standard, Sn100, and Sn110 protocols.

The assumption in image assessment is that the higher the noise value, the rougher the resulting image (Bushberg et al., 2012; Romans, 2011; SEERAM, 2016; Tack et al., 2012). This noise value is influenced by three main factors: the number of X-ray photons detected, the physical limitations of the equipment, and reconstruction parameters. In this study, the reconstruction parameters and devices used were also the same between each protocol, but there were differences in using the Tin Filter. The number or quality of X-ray photons the detector captures differs for each protocol. Suppose you look at the average noise value in Table 4.1. In that case, it can be seen that between the standard mastoid CT Scan protocol (14,060) and the Tin Filter Sn100 protocol (14,599), the values are not too different; however, in the description of the Tin Filter Sn100 protocol, it is a bit rougher. Suppose you look at the comparison between each Tin Filter protocol Sn100 (14,599), Sn110 (13,538), Sn120 (12,719), and Sn140 (12,667). In that case, the noise value decreases as the amount of energy (kV) used increases; this proves that the higher the energy (kV) used when using a Tin Filter, the lower the noise produced; this is confirmed by previous research by Yun Seok Choi in 2020 on CT Shoulder Arthrography with Tin Filter at energies of 100 kV and 140 kV with lower noise results than conventional protocols, and at an energy of 100 kV or Sn100 the radiation dose is more efficient (Choi et al., 2020), this proves that low radiation doses do not always produce high image noise, this is also the same as research by Sonja Gordic et al. in 2014 on Ultralow-Dose regarding Chest Computed Tomography in Pulmonary Nodule detection that the use of this Tin Filter can reduce the noise produced. By using a Tin Filter, the energy that passes through the Tin Filter is only high energy, so in this Tin Filter protocol, the resulting image resolution is better than the standard

protocol. Noise level indicates the radiation dose received; when using a bowtie filter or standard protocol/sign tin filter, image noise tends to be greater in the peripheral area, indicating a high local patient dose in that area (Woods & Brehm, nd). Use of Tin Filter with noise closely related to the X-ray photons used. Photon scattering is another important interaction effect in CT imaging besides photon absorption via the photoelectric effect. Photon scattering creates noise in the primary signal, and a high primary scattering ratio results in image artifacts (Woods & Brehm, nd). This is the case when many scattered photons from a short cutoff length contribute to the signal for a small number of primary photons from a long cutoff length. To increase the scatter-to-primary ratio, the number of incident photons for peripheral body parts is reduced, and thus, the number of scattered photons (Woods & Brehm, nd). Thus, this Tin Filter makes the noise between the edge and the center more homogeneous.

Next, the SNR value (signal-to-noise ratio) obtained from the HU value measured by the ROI is divided by the standard deviation of the measured ROI. This SNR value was also measured at the same 12 points as the noise, and then the SNR values from 12 points from 10 images in each protocol were averaged with the following values:

Table 1. SNR value of each Tin Filter Protocol r

Protocol	N	Average SNR	Standard Deviation	Mark Minimum	Maximum Value
Standard	10	0.4530	0.02541	0.40	0.48
sn100	10	0.4610	0.03035	0.41	0.51
Sn110	10	0.4710	0.01595	0.44	0.49
sn120	10	0.5280	0.03425	0.46	0.58
sn140	10	0.5150	0.01354	0.49	0.54

Table 3 shows the average SNR value on the standard protocol is 0.4530. The highest average SNR value on the tin filter variation protocol is on the Sn120 protocol, with an average noise value of 0.5280. The lowest average SNR value is on the Sn100 protocol of 0.4610.

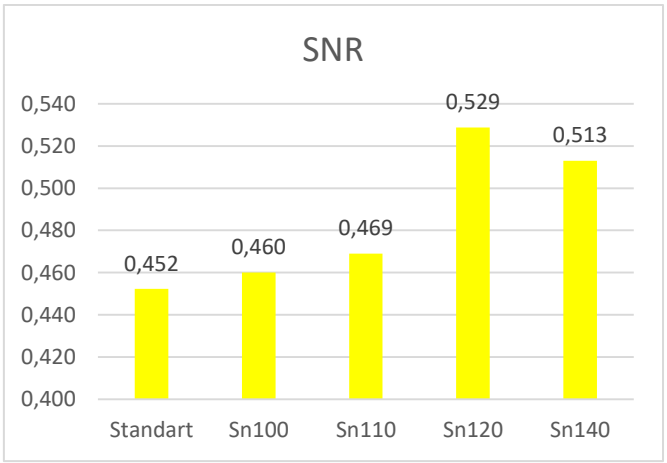

Figure 4. SNR Value Graph

Figure 6 shows that the SNR value for tin filter variations increases, with the highest SNR value being on the SN120 at 0.529 and the lowest SNR value being on the Sn100 protocol at 0.460. The SNR value for the SN100 protocol is 0.460, almost similar to the SNR value for the standard protocol, which is 0.452. From the use of tin filter variations, the SNR value also increases from Sn100 to Sn140 as the energy used increases. Furthermore, the ANOVA test on each Tin Filter protocol resulted in a sig value of 0.000<0.05, so it can be concluded that the average SNR value of

these five Tin Filter protocols is significantly **different.** Then, proceed with post hoc ANOVA to analyze each variance between groups. In this experimental research, only the average SNR value of the Standard, Sn100, and Sn110 protocols is the same, while the average SNR value of the Sn140 and Sn120 protocols is the same; thus, variable Tin Filter SNR value has two protocol groups that produce the same SNR value.

Then, proceed with post hoc ANOVA to analyze each variance between groups. In this experimental research, only the average SNR value of the Standard, Sn100, and Sn110 protocols is the same, while the average SNR value of the Sn140 and Sn120 protocols is the same; thus, variable Tin Filter SNR value has two protocol groups that produce the same SNR value.

The SNR value better reflects the signal from each image pixel, the average background signal value, and the deviation from the uniform background in the image. The higher the SNR value, the better the image quality (Bushberg et al., 2012; El-Khoury et al., 2004; Romans, 2011; SEERAM, 2016; Tack et al., 2012). The SNR value in this study is in Table 4.2 in the standard protocol (0.453), and the t in protocol f filter Sn100 (0.461). The value is not too different, but the SNR value of the Tin Filter Sn100 protocol is higher than the standard protocol. If we look at each Tin Filter protocol Sn100 (0.461), Sn110 (0.471), Sn120 (0.528), and Sn140 (0.515), the SNR value is higher; this proves that the higher the energy (kV) used will increase the value. The resulting SNR. This is supported by previous research by Andrea Agostini et al. in 2020 regarding third-generation interactive reconstruction with high pitch, low dose Thorax CT Scan protocol with Tin Filter for beamforming at 100 kV with the result that the SNR value increased in the protocol using Tin Filter (Agostini et al., 2021), and in research by Patricia Dewes et al., in 2016 regarding Low-dose Abdominal CT Scan for the detection of stones in the urinary tract - the effect of adding spectral shaping results in an increase in the SNR value in the protocol that uses the Tin Filter, it will, but at Sn150 energy the values are not significantly different. This proves that at energies of 140 kV and above, there will be a decrease in the SNR value, the same as in this research on Sn140; the SNR value also decreased. The SNR value in Holger Haubenreisser's research, 2015 regarding the CT Scan of the Thorax on the third generation dual-source CT Scan using a tin filter for spectral shaping at 100 kVp, stated that the SNR value increased in parts of the Aorta, Adipose tissue Lung, Trachea, but in the Supraspinatus muscle does not increase. This increase in the SNR value is important to assess because SNR is one of the most meaningful metrics that describes the conspicuity of an object or how well it will appear to an observer (Bushberg et al., 2012).

After measuring the noise and SNR values, the radiation dose recorded from the results of scanning the water phantom in the form of CTDIvol and DLP is recorded as follows:

Table 2. Radiation Dose Results from Each Tin Filter Protocol

Protocol	CTDIvol	DLP
Standard	16.71	110
Sn100	9.70	81
Sn110	13.42	113
sn120	16.53	139
sn140	20,24	170

In Table 5, each CTDIvol radiation dose produced using the tin filter variation protocol tends to increase from Sn100 to Sn140, with the lowest CTDIvol result being in the Sn100 protocol at 9.70 and the highest CDTIvol result being in the SN140 protocol at 20. .24 . From the results of the

recorded radiation dose, it can be seen that the standard/no tin filter protocol tends to be greater, namely 16.71, compared to the Sn100 protocol of 9.70.

After analyzing the recorded noise, SNR, and radiation dose values, proceed with analyzing the NPS (noise power spectrum) with indoQCT software version 22 by uploading an image that represents the results of the water phantom scanning, namely on slice number 66, which is at the middle level of the water phantom in each standard protocol, Sn100, Sn110, Sn120, and Sn140. This NPS value is obtained from the ROI in a homogeneous area shown in Figure 7,

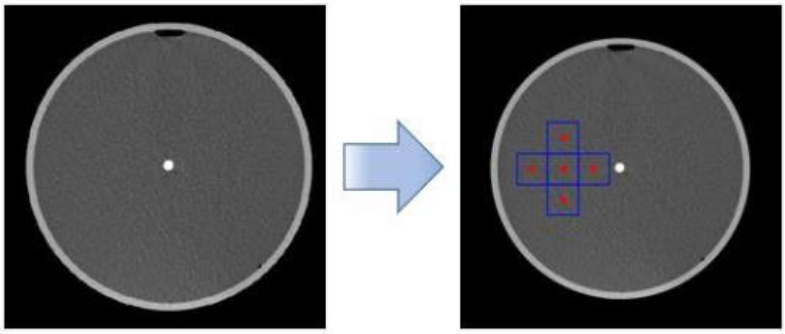

Figure 5. ROI area in IndoQCT software

Then, the ROI of each protocol is stored in the form of a 300x300 pixel cropped square shown in Figure 8. This is done to assess the characteristics of the noise by assessing the resulting texture noise in more detail.

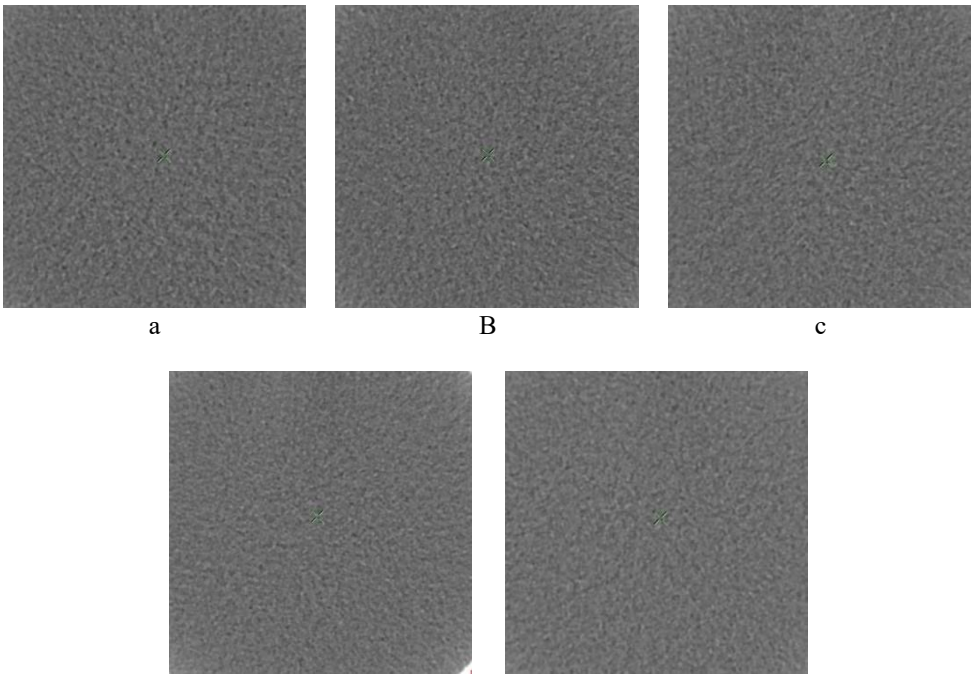

Figure 6. Results: Each protocol's sample image is cut to 300 x 300 pixels. a). Standard, b). Sn100, c). Sn110, d). Sn120 and e). sn140

Next, NPS measurements were carried out by carrying out a Fourier transformation on the average pixel value in each ROI. Fourier transformation is a model that moves the spatial or time domains into the frequency domain. Fourier transformation is a process widely used to move the

domain of a function or object into the frequency domain, and then after carrying out the Fourier transformation, it produces a 2-dimensional image, which can be seen in Figure 9. The 2-dimensional image in the image shows the texture of the focus point, which varies in each image.

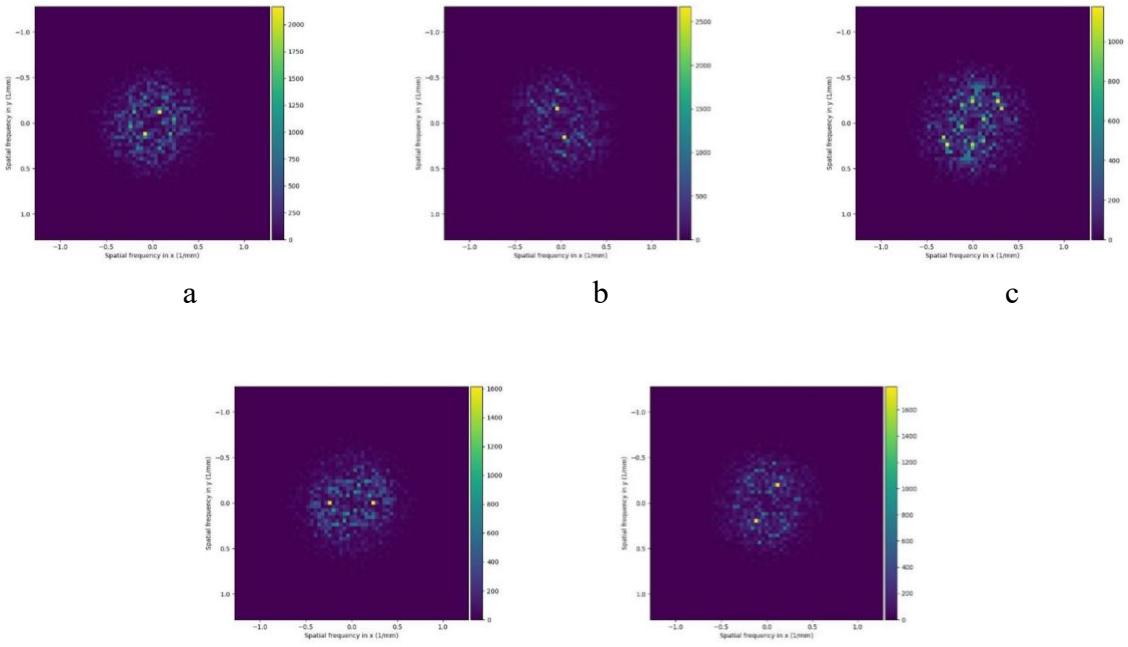

a b c

d e

Figure 7. 2D image results from the Fourier transform of the average pixel in each ROI . a). Standard, b). Sn100, c). Sn110, d). Sn120 and e). Sn140

After uploading an image of the water phantom results and putting the ROI on the image, click calculate. Then, the results can be saved, as shown in Figure 10. Then, the NPS calculation results from the IndoQCT software can be exported in Excel format. The following is a recap of the NPS results in Table 6 :

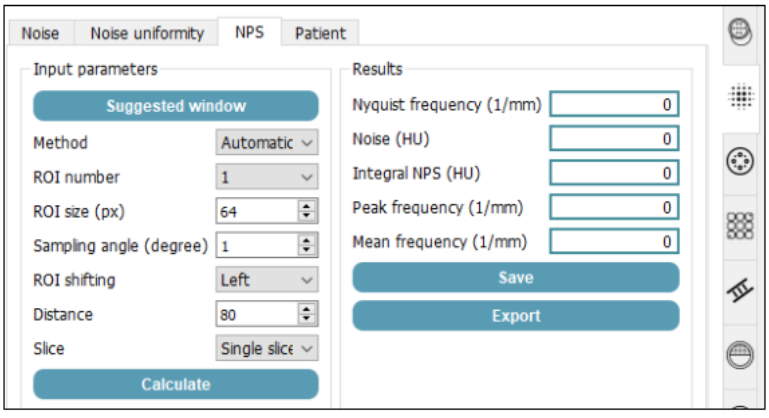

Figure 8. IndoQCT displays NPS calculations

Table 3. NPS value of each *Tin* Filter Protocol

Protocol	Frequency	Peak NPS Value
Standard	0.28	430.65
Sn100	0.2	391.80
Sn110	0.28	255.52

Protocol	Frequency	Peak NPS Value
Sn120	0.28	330.89
Sn140	0.28	253.74

From Table 6, it can be seen that among all the protocols, the frequency is 0.28, but the Sn100 protocol is at a frequency of 0.2, and this difference is not too big. Of each protocol used, the standard protocol has the highest peak value and decreases as the energy used increases. The highest peak value was 430.65 in the standard protocol/without tin filter, and the lowest was in Sn140, with a value of 253.74. The NPS value data from the IndoQCT software is exported in Excel format, and then a graph is created as below:

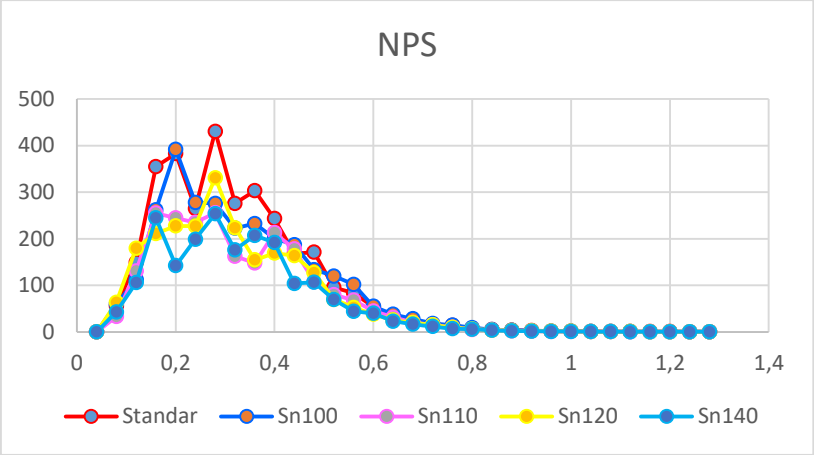

Figure 9. Graph of NPS Values for Each *Tin* Filter Protocol

If simplified by just selecting the *peak* NPS value, it would be as follows:

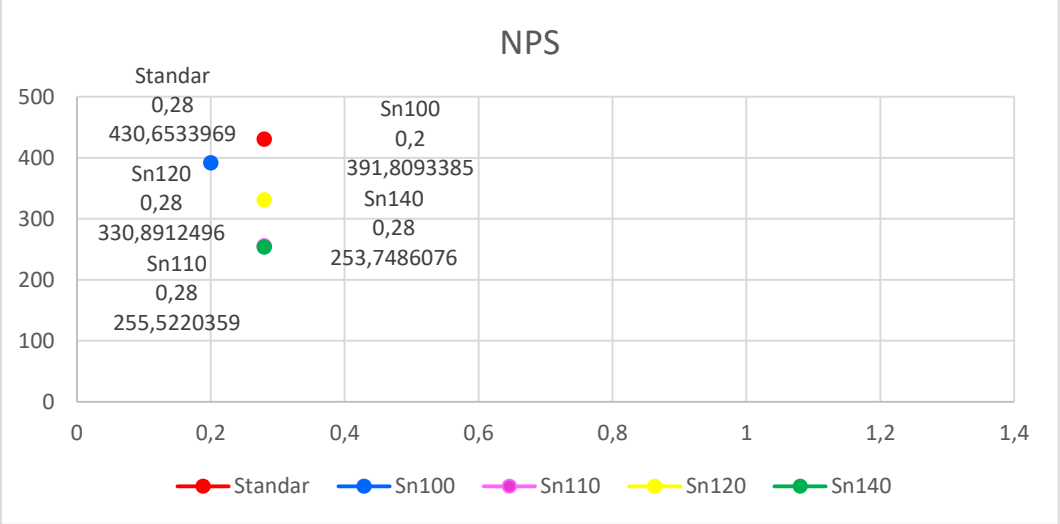

Figure 10. Peak NPS Value of Each Tin Filter Protocol

The noise power spectrum can generally describe the noise properties of an imaging system. This NPS is a more comprehensive description than the standard deviation of a pixel or what we know as image noise value. This NPS explains the characteristics of the magnitude and spatial frequency of noise in CT scan images, which plays an important role in analyzing and optimizing the imaging system's performance. This NPS is most often associated with other parameters to assess image quality, and this NPS has been commonly used in the development, characterization, optimization,

and comparison of various new imaging technologies. The tin filter protocol analyzes the NPS value from the scanning water phantom using IndoQCT version 22 software. This software is very simple in application and easy to understand for new users. This software has been used in various research, such as research on automatic validation of gantry tilt (Noviliawati et al., 2021), research on automation of CT Number linearity measurements on ACR phantoms (Anam et al., 2023), research on evaluating automatic measurement of slice profile sensitivity (Widyanti et al., 2023), and research on the comparison of NPS and MTF in iterative reconstruction and deep learning reconstruction (Setiawan et al., 2023). The first step in the IndoQCT software is to upload images from each research protocol. From the initial image (spatial domain), it is converted into a frequency domain in the form of a 2D image that has been Fourier transformed as in Figure 4.5; the difference in the 2D image at a glance is not that big. The difference is visible. The 2D image results in each protocol are still in good condition because the 2D noise spectrum image has a tight focus point. Figure 13 below shows a good reference noise spectrum image. The further to the left the image the noise spectrum is, the lower the CT scan equipment used in this research is still in good condition.

The peak value is in the standard protocol, but each of these protocols is at almost the same frequency, except for the Tin Filter Sn100 protocol, which is at a frequency of 0.2. The relationship between frequency and NPS value is that the higher the frequency, the noise produced, the lower it will be, or in other words, the better the texture noise produced (Bushberg et al., 2012; SEERAM, 2016). If we look at graphs 4.9 and 4.10, the graphs are almost similar in shape to the standard protocol / without a tin filter, namely the Tin Filter Sn100 protocol.

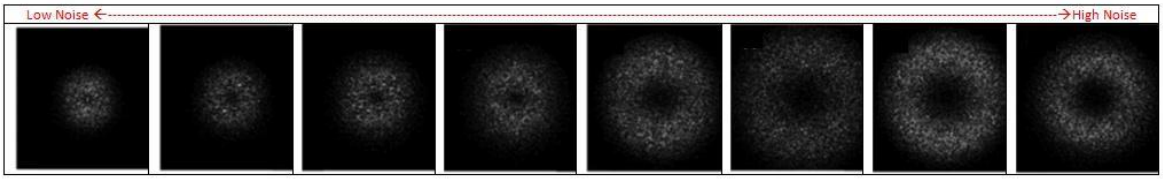

Figure 11. Noise Level Reference

After analyzing the value of noise, SNR, and NPS on the water phantom, the best protocol was chosen with a noise level that was almost similar to the standard protocol (14.0600 vs. 14.5990) but with a much-reduced dose than the standard protocol (16.71 vs. 9.70), namely the tin filter protocol Sn100 and the SNR value is close to the standard value (0.4530 vs. 0.4610) and the texture noise or NPS is at an almost similar frequency (0.28 vs. 0.20).

Noise, SNR, and NPS analysis on this water phantom image found that the Tin Filter Sn100 protocol is very good compared to the others, taking into account the noise value, which has the highest value (14,599) compared to the Tin Filter Sn110 protocol (13,538), Sn120 (12,719) and Sn140 (12,667). The Sn100 protocol is most similar to the standard protocol (14.06), but a low or high noise value is not a guarantee that the CT scan image produced is good or not, but the noise value is a reference for the image to be able to diagnose a pathological disorder or not. In the post hoc ANOVA analysis, the noise value proves that the noise value in the Sn140 and Sn120 protocols is the same, so the effect of the tin filter on the noise value only affects Sn100 and Sn110. In the Analysis of the SNR value, this SNR reflects an original picture of the object. The higher the SNR value, the better it reflects the original object; the SNR value in the protocol Sn100 (0.463), Sn110 (0.471), Sn120 (0.52), and The Sn140 (0.515) increases as the number of energy increases, but when using Sn140 the SNR value drops and in the post hoc anova analysis there are two groups of protocols that produce the same SNR, namely Standard, Sn100 and Sn110 vs. Sn120 and Sn140 and at Analysis of the Sn100

NPS value has a slight difference with the standard protocol in terms of frequency, in the standard protocol it is at a frequency of 0.28 and in the Tin Filter Sn100 protocol it is at a frequency of 0.2. However, the noise produced is still better than the standard protocol, and the most important aspect is the radiation dose; from the standard protocol to the Tin Filter Sn100 protocol, the radiation dose is reduced by 41.95%. This is similar to previous research by K. Kimura et al. in 2022 regarding the radiation dose and diagnostic performance of using Tin filters in colorectal cancer patients on the Tin Filter Sn100 protocol, which can substantially reduce the radiation dose by 89%, but the area scanned for abdominal organs so that these different density levels will affect the penetrating power of X-ray photons that reach the detector. Therefore, the Sn100 protocol was chosen and tested again on a rando phantom object; this rando phantom has specifications similar to real humans, and its attenuation level is equivalent to tissue for X-ray diagnostics (Shrimpton et al., 1981). With the above considerations, the Sn100 protocol was tested with a different scanning object, namely the rando phantom object whose specifications are very similar to real humans; this phantom has been used in several studies, including research by Ulla Nikupaavo et al. in 2015, regarding Lens Dose in Routine Head CT: comparing the differences between optimization methods and Anthropomorphic Phantoms or phantom rando, with the result that gantry tilting can reduce the radiation dose to the eye lens (Serhal et al., 2001) and research on radiation dose by Charbel Bou Serhal et al. in 2001 by utilizing this type of phantom as a scanning object (Serhal et al. ., 2001) The results of the Rando phantom scanning are shown in three image slices which represent the results of the Sn100 protocol scanning at the base, mid and apex levels of the temporal bone as shown in Figure 14.

Figure 12. Mastoid Air Cell Scanning Results in the Protocol Tin Filter Sn100 with Phantom Rando Object

Then, the image results were assessed subjectively by asking seven questions by two radiologists with more than ten years of experience. About image quality, noise, sharpness, anatomical boundaries, anatomical parts of the cochlear apical turn, malleus incus, and cochlear nerve opening. This subjective assessment is carried out using a Totoku brand medical grade monitor screen with a reference to the image to be assessed as in Figure 15.

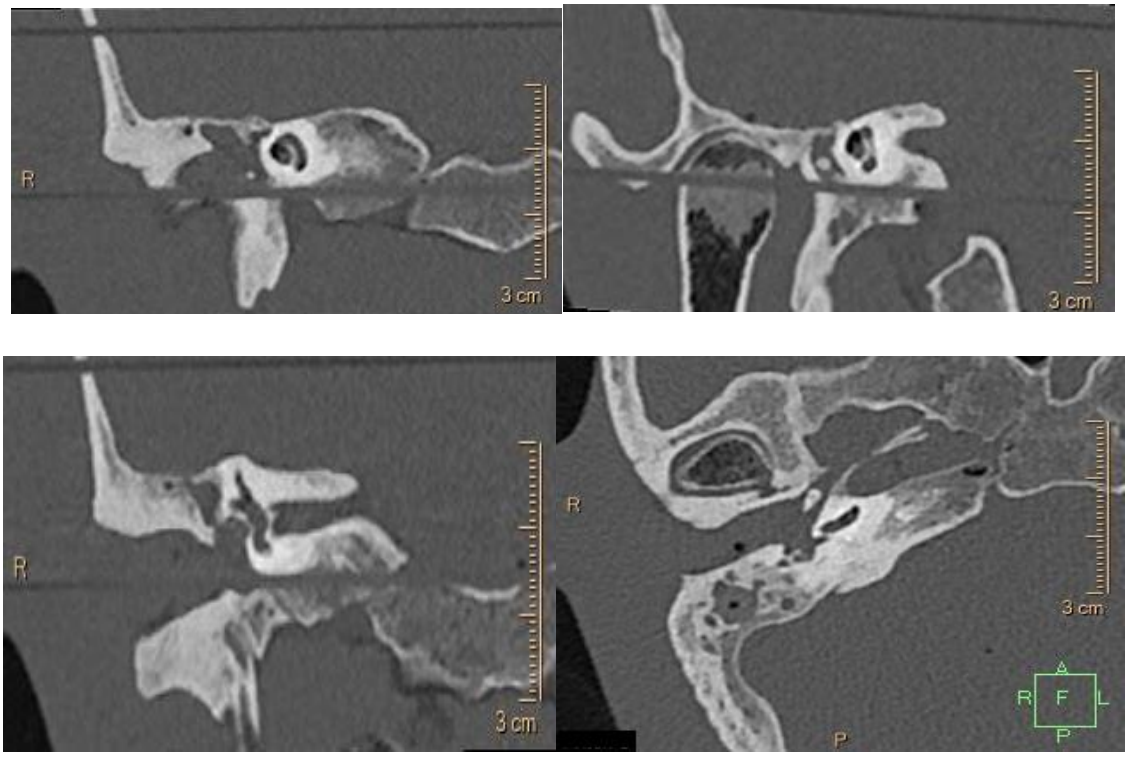

Figure 15. 1Reference to the mastoid image in the questionnaire

However, complete image data is also provided for processing in MPR mode to maximize assessment. The following is a recap of the subjective assessment results by two respondents, which are shown in the table below:

Table 6. Recap of Subjective Assessment Questionnaire Data from 7 Questions

Respondents	Question							Total
	1	2	3	4	5	6	7	
Radiologist 1	4	5	4	5	3	4	5	30
Radiologist 2	4	5	4	5	4	4	5	31

In table 6 the first question about image quality from the two radiologists gave a score of 4 meaning that the two radiologists agreed that there were few artifacts but were able to show anatomical structures in detail, in the second question about the noise produced the two radiologists gave a score of 5 meaning the picture produced is Excellent Image without artifacts and clearly shows the anatomical structure in detail, on the third question about the sharpness of the image the two radiologists gave a score of 4 meaning that there were few artifacts but were able to show the anatomical structure in detail, on the fourth question about the anatomical boundaries the two radiologists gave a score of 5 meaning Excellent Image without artifacts and clearly shows the anatomical structure in detail, on the fifth question about the coclear apical turn anatomy the two radiologists gave a different score i.e. 3 means that there are artifacts but not significant but can still show anatomical structures well and can still be diagnosed , while radiologist 2 gives a score of 4 meaning that there are few artifacts but are able to show anatomical structures in detail , on the sixth question about the anatomy of the malleus incuss the two radiologists give score 4 and on the seventh cochlear nerve opening question both radiologists gave a score of 5 meaning Excellent image without artefacts and clearly shows the anatomical structure in detail . Overall, the subjective assessment of the two radiologists agreed that the mastoid CT scan protocol with Sn100 could provide better and

more informative image quality results so that it could assist radiologists in making a diagnosis. The resulting kappa value is 0.75 with a significant value of 0.013, indicating that the coefficient value indicates a correlation or level of agreement at a moderate level (McKenzie & Mahnken, 2023). subjectively, namely noise, sharpness, anatomical boundaries, and the smallest anatomical parts, namely the cochlear apical turn, malleus incus, and cochlear nerve opening. The anatomical parts assessed by the observer are very important in supporting guiding surgery in the installation of cochlear implants, so high-resolution images are needed here (Rodrigues et al., 2020). This mastoid CT scan image was also used in research by Henrique Rodrigues, 2020 regarding Mastoid, middle ear, and inner ear analysis on CT scan – possible contribution to cadaver identification, with CT scan imaging of the Mastoid in visual assessment of the mastoid examination proving to be a powerful and reliable approach to identify unique bone features and contribute to human identification. In research by Khalid Hindi et al. in 2014 regarding Mastoid pneumatization of mastoid air cells and other parts of the temporal bone, it was recorded as symmetrical in more than 75%. Pre-operative assessment of the temporal bone and PNS with a CT scan can help evaluate anatomical landmarks and reduce the possibility of surgical complications because the image can clearly show the 3D structure (Hindi et al., 2014). Level of resolution on CT Scan This Mastoid needs to be improved. Therefore, using a Tin Filter is a must to improve image quality. In the future, imaging technologies should be developed to non-invasively assess the structure and physiology of the middle ear/eustachian tube in relation to their role in the pathogenesis of otitis media (Alper et al., 2017).

This Tin Filter was widely used in various examinations, such as in previous research by Katharina Martini in 2015 (Martini et al., 2015) on the thorax protocol; it was proven that the tin filter combined with iterative reconstruction was effective in detecting solid and non-solid nodules with a specificity of 85 .7% and in research by Andrew D. McQuiston et al., in 2016 the ability to detect the amount of calcium in coronary blood vessels using the Sn100 protocol was proven to be accurate in quantifying calcium scoring without correction for the HU threshold and in research by Yun Seok Choi et al., in 2020 (Choi et al., 2020) in an arthrography examination proved that the use of the Sn100 and Sn140 tin filter protocols was proven to reduce radiation dose by 70% and 60% compared to the usual conventional protocol without reducing image quality.

The Tin Filter protocol is very useful in mastoid CT scan examinations because it is proven to reduce the radiation dose from the standard protocol/without tin filter to the Sn100 protocol by 41.95%, and the resulting image quality is quite good with noise values that are not much different and sufficient to diagnostic needs and again the noise generated by this protocol is still within reasonable limits because the increase in noise produced by this Tin Filter variation is not too high compared to the standard protocol/without tin filter, so this Tin Filter protocol can be used as a permanent protocol and set as an inspection SOP Mastoid CT Scan at Hermina Hospital Depok. The limitation of this research is that it cannot be carried out directly on patients because it must consider the radiation dose given during the examination, and in testing with a rando phantom, the pneumatization image of the mastoid organ is not visible well because the preservation process in the phantom so that the cavities in the Mastoid are already filled. Fluid.

CONCLUSION

Based on the results of research to analyze the level of noise and reduction in radiation dose produced in each variation of the tin filter in the mastoid CT scan protocol which will be used as a reference in making SOPs, it can be concluded that there are differences in the level of noise produced in each variation of the Tin Filter (Sn100, Sn110, Sn120 and Sn140) given in the mastoid protocol

with a p-value (p <0.05) of 76.330 and there was a reduction in radiation dose from the standard protocol to the Tin filter Sn100 protocol of 41.95%. The noise value decreases as the amount of energy (kV) used increases; this proves that the higher the energy (kV) used when using a Tin Filter, the lower the noise produced. The higher the energy (kV) used in the Tin Filter protocol, the higher the SNR value produced; however, at Sn140, the SNR value decreases so that at energies of 120 kV and above, this Tin Filter has a certain tolerance limit. The highest NPS peak value is in the standard protocol/without tin filter and decreases with the energy used, but each of these protocols is at almost the same frequency, except for the Tin Filter Sn100 protocol, which is at a frequency of 0.2. This means that the resulting texture noise is similar. The radiation dose resulting from the Standard Protocol/without tin filter, the CTDIvol radiation dose was 16.71 mGy with a DLP value of 110 mGy.cm; in the Tin Filter Sn100 Protocol the CTDIvol radiation dose was 9.70 mGy with a DLP value of 81 mGy.cm, in the Protocol The Tin Filter Sn110 radiation dose is 13.42 CTDIvol with a DLP value of 113 mGy.cm, in the Tin Filter Sn120 Protocol the radiation dose is 16.53 CTDIvol with a DLP value of 139 mGy.cm and in the Tin Filter Sn140 Protocol the radiation dose is 20.24 CTDIvol mGy with a DLP value of 170 mGy.cm. The higher the energy used, the lower the radiation dose produced using a Tin Filter. The image quality of the phantom rando object is of good quality and can show small anatomical structures such as the anatomical parts of the cochlear apical turn, malleus incus, and cochlear nerve opening. The results of the kohen kappa between the two respondents show a kappa value of 0.75 with a significant value of 0.013, indicating that the coefficient value indicates a correlation or level of agreement at a moderate level. Overall, the two radiologists agreed that the CT Scan Mastoid examination protocol with Sn100 can provide good image quality results and assist in making a diagnosis.

REFERENCES

Agostini, A., Borgheresi, A., Carotti, M., Ottaviani, L., Badaloni, M., Floridi, C., & Giovagnoni, A. (2021). Third-generation iterative reconstruction on a dual-source, high-pitch, low-dose chest CT protocol with tin filter for spectral shaping at 100 kV: a study on a small series of COVID-19 patients. *Radiologia Medica*, *126*(3), 388–398. https://doi.org/10.1007/s11547-020-01298-5

Alper, C. M., Luntz, M., Takahashi, H., Ghadiali, S. N., Swarts, J. D., Teixeira, M. S., Csákányi, Z., Yehudai, N., Kania, R., & Poe, D. S. (2017). Panel 2: Anatomy (Eustachian Tube, Middle Ear, and Mastoid—Anatomy, Physiology, Pathophysiology, and Pathogenesis). *Otolaryngology - Head and Neck Surgery (United States)*, *156*(4_suppl), S22–S40. https://doi.org/10.1177/0194599816647959

Anam, C., Amilia, R., Naufal, A., Budi, W. S., Maya, A. T., & Dougherty, G. (2023). The automated measurement of CT number linearity using an ACR accreditation phantom. *Biomedical Physics and Engineering Express*, *9*(1), 17002. https://doi.org/10.1088/2057-1976/aca9d5

Braun, F. M., Johnson, T. R. C., Sommer, W. H., Thierfelder, K. M., & Meinel, F. G. (2015). Chest CT using spectral filtration: radiation dose, image quality, and spectrum of clinical utility. *European Radiology*, *25*(6), 1598–1606. https://doi.org/10.1007/s00330-014-3559-1

Bushberg, J. T., Seibert, J. A., Leidholdt, E. M., Boone, J. M., & Goldschmidt, E. J. (2012). The Essential Physics of Medical Imaging. In *Medical Physics* (Vol. 30, Issue 7). https://doi.org/10.1118/1.1585033

Choi, Y. S., Choo, H. J., Lee, S. J., Kim, D. W., Han, J. Y., & Kim, D. S. (2020). Computed tomography arthrography of the shoulder with tin filter-based spectral shaping at 100 kV and 140 kV. *Acta Radiologica*. https://doi.org/10.1177/0284185120965551

Dexian Tan, A., Ng, J. H., Lim, S. A., Low, D. Y. M., & Yuen, H. W. (2018). Classification of Temporal Bone Pneumatization on High-Resolution Computed Tomography: Prevalence Patterns and Implications. *Otolaryngology - Head and Neck Surgery (United States)*, *159*(4),

743–749. https://doi.org/10.1177/0194599818778268

El-Khoury, G. Y., Bennett, D. L., & Ondr, G. J. (2004). Multidetector-row computed tomography. In *Journal of the American Academy of Orthopaedic Surgeons* (Vol. 12, Issue 1). https://doi.org/10.1007/b139071

Ertel, D., Lell, M. M., Harig, F., Flohr, T., Schmidt, B., & Kalender, W. A. (2009). Cardiac spiral dual-source CT with high pitch: A feasibility study. *European Radiology*, *19*(10), 2357–2362. https://doi.org/10.1007/s00330-009-1503-6

Hamann, A., Di, H. C., & Crm, C. T. (2017). *Tin Filter spectral shaping – a demonstration of Agatston equivalence*.

Hindi, K., Alazzawi, S., Raman, R., Prepageran, N., & Rahmat, K. (2014). Pneumatization of Mastoid Air Cells, Temporal Bone, Ethmoid and Sphenoid Sinuses. Any Correlation? *Indian Journal of Otolaryngology and Head and Neck Surgery*, *66*(4), 429–436. https://doi.org/10.1007/s12070-014-0745-z

Kalmar, P. I., Quehenberger, F., Steiner, J., Lutfi, A., Bohlsen, D., Talakic, E., Hassler, E. M., & Schöllnast, H. (2014). The impact of iterative reconstruction on image quality and radiation dose in thoracic and abdominal CT. *European Journal of Radiology*, *83*(8), 1416–1420. https://doi.org/10.1016/j.ejrad.2014.05.017

Kimura, K., Fujioka, T., Mori, M., Adachi, T., Hiraishi, T., Hada, H., Ishikawa, T., & Tateishi, U. (2022). Dose Reduction and Diagnostic Performance of Tin Filter–Based Spectral Shaping CT in Patients with Colorectal Cancer. *Tomography*, *8*(2), 1079–1089. https://doi.org/10.3390/tomography8020088

Kovalchuk, A., & Kolb, B. (2017). Low dose radiation effects on the brain–from mechanisms and behavioral outcomes to mitigation strategies. *Cell Cycle*, *16*(13), 1266–1270. https://doi.org/10.1080/15384101.2017.1320003

Lell, M. M., May, M. S., Brand, M., Eller, A., Buder, T., Hofmann, E., Uder, M., & Wuest, W. (2015). Imaging the parasinus region with a third-generation dual-source CT and the effect of tin filtration on image quality and radiation dose. *American Journal of Neuroradiology*, *36*(7), 1225–1230. https://doi.org/10.3174/ajnr.A4270

Lell, M., Marwan, M., Schepis, T., Pflederer, T., Anders, K., Flohr, T., Allmendinger, T., Kalender, W., Ertel, D., Thierfelder, C., Kuettner, A., Ropers, D., Daniel, W. G., & Achenbach, S. (2009). Prospectively ECG-triggered high-pitch spiral acquisition for coronary CT angiography using dual source CT: Technique and initial experience. *European Radiology*, *19*(11), 2576–2583. https://doi.org/10.1007/s00330-009-1558-4

Leschka, S., Stolzmann, P., Desbiolles, L., Baumueller, S., Goetti, R., Schertler, T., Scheffel, H., Plass, A., Falk, V., Feuchtner, G., Marincek, B., & Alkadhi, H. (2009). Diagnostic accuracy of high-pitch dual-source CT for the assessment of coronary stenoses: First experience. *European Radiology*, *19*(12), 2896–2903. https://doi.org/10.1007/s00330-009-1618-9

Magnuson, B. (2003). Functions of the mastoid cell system: Auto-regulation of temperature and gas pressure. *Journal of Laryngology and Otology*, *117*(2), 99–103. https://doi.org/10.1258/002221503762624512

Mannudeep K. Kalra, Michael M. Maher, Thomas L. Toth, Bernhard Schmidt, Bryan L. Westerman, Hugh T. Morgan, S. S. (2004). Techniques and Applications of Automatic Tube Current Modulation for CT1 Introduction. *RSNA*.

Martini, K., Higashigaito, K., Barth, B. K., Baumueller, S., Alkadhi, H., & Frauenfelder, T. (2015). Ultralow-dose CT with tin filtration for detection of solid and sub solid pulmonary nodules: A phantom study. *British Journal of Radiology*, *88*(1056). https://doi.org/10.1259/bjr.20150389

McKenney, S. E., Seibert, J. A., Lamba, R., & Boone, J. M. (2014). Methods for CT automatic exposure control protocol translation between scanner platforms. *Journal of the American College of Radiology*, *11*(3), 285–291. https://doi.org/10.1016/j.jacr.2013.10.014

McKenzie, K. A., & Mahnken, J. D. (2023). Simulating and estimating agreement in the presence of multiple raters and covariates. *Statistics in Medicine*, *42*(11), 1687–1698. https://doi.org/10.1002/sim.9694

Mcnitt-gray, M. (2011). Tube Current Modulation Approaches : Overview , Practical Issues and Potential Pitfalls Tube Current Modulation - Overview. *Current*.

Mozaffary, A., Trabzonlu, T. A., Kim, D., & Yaghmai, V. (2019). Comparison of tin filter–based spectral shaping CT and low-dose protocol for detection of urinary calculi. *American Journal of Roentgenology*, *212*(4), 808–814. https://doi.org/10.2214/AJR.18.20154

Noviliawati, R., Anam, C., Sutanto, H., Dougherty, G., & Mak'ruf, M. R. (2021). Automatic validation of the gantry tilt in a computed tomography scanner using a head polymethyl methacrylate phantom. *Polish Journal of Medical Physics and Engineering*, *27*(1), 57–62. https://doi.org/10.2478/pjmpe-2021-0008

Rajendran, K., Voss, B. A., Zhou, W., Tao, S., Delone, D. R., Lane, J. I., Weaver, J. M., Carlson, M. L., Fletcher, J. G., McCollough, C. H., & Leng, S. (2020). Dose Reduction for Sinus and Temporal Bone Imaging Using Photon-Counting Detector CT with an Additional Tin Filter. *Investigative Radiology*, *55*(2), 91–100. https://doi.org/10.1097/RLI.0000000000000614

Rodrigues, H., Ramos, R., Fagundes, L., Galego, O., Navega, D., Coelho, J. d. O., Alves, F. C., & Cunha, E. (2020). Mastoid, middle ear and inner ear analysis in CT scan – a possible contribution for the identification of remains. *Medicine, Science and the Law*, *60*(2), 102–111. https://doi.org/10.1177/0025802419893424

Romans, L. E. (2011). *Computed Tomography for Technologist*. Wolters Kluwer Health.

Schüle, S., Strobel, J. R. B., Lorenz, K. J., Beer, M., & Hackenbroch, C. (2023). Tin filter compared to low kV protocols - optimizing sinonasal imaging in computed tomography. *PLoS ONE*, *18*(1 January), 1–13. https://doi.org/10.1371/journal.pone.0279907

SEERAM, E. (2016). *COMPUTED TOMOGRAPHY Physical Principles, Clinical Applications, and Quality Control* (FOURTH). Elsevier.

Serhal, C. B., Jacobs, R., Gijbels, F., Bosmans, H., Hermans, R., Quirynen, M., & Van Steenberghe, D. (2001). Absorbed doses from spiral CT and conventional spiral tomography: A phantom vs. Cadaver study. *Clinical Oral Implants Research*, *12*(5), 473–478. https://doi.org/10.1034/j.1600-0501.2001.120507.x

Setiawan, A. M. B., Anam, C., Hidayanto, E., Sutanto, H., Naufal, A., & Dougherty, G. (2023). Comparison of noise-power spectrum and modulation-transfer function for CT images reconstructed with iterative and deep learning image reconstructions: An initial experience study. *Polish Journal of Medical Physics and Engineering*, *29*(2), 104–112. https://doi.org/10.2478/pjmpe-2023-0012

Shrimpton, P. C., Wall, B. F., & Fisher, E. S. (1981). The tissue-equivalence of the Alderson Rando anthropomorphic phantom for X-rays of diagnostic qualities. *Physics in Medicine and Biology*, *26*(1), 133–139. https://doi.org/10.1088/0031-9155/26/1/013

Singh, S., Kalra, M. K., Gilman, M. D., Hsieh, J., Pien, H. H., Digumarthy, S. R., & Shepard, J.-A. O. (n.d.). Adaptive Statistical Iterative Reconstruction Technique for Radiation Dose Reduction in Chest CT: A Pilot Study 1. *Radiology*, *259*. https://doi.org/10.1148/radiol.11101450/-/DC1

Sowby, F. D. (1981). ICRP Statement on Tissue Reactions and Early and Late Effects of Radiation in Normal Tissues and Organs – Threshold Doses for Tissue Reactions in a Radiation Protection Context. *Annals of the ICRP*, *6*(1), 1. https://doi.org/10.1016/0146-6453(81)90127-5

Tacelli, N., Remy-Jardin, M., Flohr, T., Faivre, J. B., Delannoy, V., Duhamel, A., & Remy, J. (2010). Dual-source chest CT angiography with high temporal resolution and high pitch modes: Evaluation of image quality in 140 patients. *European Radiology*, *20*(5), 1188–1196. https://doi.org/10.1007/s00330-009-1638-5

Tack, D., Kalra, M. K., & Gevenois, P. A. (2012). *Radiation Dose from Multidetector CT*. https://doi.org/10.1007/987-3-642-24535-0

Widyanti, E. R., Anam, C., Hidayanto, E., Naufal, A., & Haekal, M. (2023). An evaluation of automated measurement of slice sensitivity profile of computed tomography image: Field of view variations. *Indonesian Journal of Electrical Engineering and Computer Science*, *29*(3), 1430–1437. https://doi.org/10.11591/ijeecs.v29.i3.pp1430-1437

Woods, M., & Brehm, M. (n.d.). *Shaping the beam Versatile filtration for unique diagnostic potential within Siemens Healthineers CT*.

Zhang, G. M. Y., Shi, B., Sun, H., Xue, H. D., Wang, Y., Liang, J. X., Xu, K., Wang, M., Wang, M., Xu, M., & Jin, Z. Y. (2017). High-pitch low-dose abdominopelvic CT with tin-filtration technique for detecting urinary stones. *Abdominal Radiology*, *42*(8), 2127–2134. https://doi.org/10.1007/s00261-017-1103-x